

NJC

Accepted Manuscript



This is an *Accepted Manuscript*, which has been through the Royal Society of Chemistry peer review process and has been accepted for publication.

Accepted Manuscripts are published online shortly after acceptance, before technical editing, formatting and proof reading. Using this free service, authors can make their results available to the community, in citable form, before we publish the edited article. We will replace this *Accepted Manuscript* with the edited and formatted *Advance Article* as soon as it is available.

You can find more information about *Accepted Manuscripts* in the [Information for Authors](#).

Please note that technical editing may introduce minor changes to the text and/or graphics, which may alter content. The journal's standard [Terms & Conditions](#) and the [Ethical guidelines](#) still apply. In no event shall the Royal Society of Chemistry be held responsible for any errors or omissions in this *Accepted Manuscript* or any consequences arising from the use of any information it contains.

Aerosol-assisted synthesis of mesoporous aluminosilicate microspheres: the effect of the aluminum precursor

Sonia Fiorilli^a, Valentina Cauda^b, Lucia Pontiroli^{a,c}, Chiara Vitale-Brovarone^a, Barbara Onida^{a*}

^a Dipartimento di Scienza Applicata e Tecnologia, Politecnico di Torino, Corso Duca degli Abruzzi 24, 10129 Torino, Italy

^b Center for Space Human Robotics - IIT@PoliTO, Istituto Italiano di Tecnologia, Corso Trento 21 10129 Torino, Italy

^c Division of Oral Biology, University of Leeds School of Dentistry, St. James's University Hospital, Leeds LS9 7TF, United Kingdom

*Corresponding author: Tel: +39 011 0904631; E-mail: barbara.onida@polito.it

Keywords: spray-drying, aluminosilicates, mesoporous, micro-spheres, Brønsted/Lewis acidity

Abstract

The development of a cost-effective process for the production of mesostructured aluminosilicates, with high Al content and controlled morphology, is highly desired. In this work, mesoporous aluminosilicate, with spherical morphology, have been synthesized under mild acidic aqueous conditions by using an aerosol-assisted sol-gel process, a simple, versatile and potentially scalable method. Two aluminum sources, aluminum isopropoxide and aluminum chloride, have been used, keeping constant the other synthesis and process parameters. FE-SEM, coupled to EDX, TEM and N₂ adsorption-desorption measurements have shown that sprayed powders consist of microspheres, homogeneous in size, and characterized by high surface area (up to 640 m²/g) and narrow pore size distribution (centred at 2.5 nm). ²⁷Al-NMR spectra of as-synthesized samples have evidenced mostly tetrahedral Al, also for the sample with higher Al content (Si/Al =5.7). The surface acidity of the sprayed samples has been investigated by FT-IR spectroscopy of adsorbed ammonia and CO adsorption, which has shown the presence of Brønsted sites (able to protonate ammonia) and of weak Lewis sites.

1. Introduction

Heterogeneous solid acid catalysts are widely used for fine chemical reactions [1, 2], alkylation of aromatic hydrocarbons [3] and cracking vacuum gas oil [4, 5]. The most commonly used catalysts for all these applications belong to the crystalline microporous zeolites family. However, the narrow pore size of zeolitic supports strongly limits the diffusion and conversion of large molecules, making the design and the optimization of large-pore acidic catalysts still a great challenge in the materials science field. To this aim, a wide variety of synthetic strategies have been proposed to obtain solids with enhanced diffusion and stable acidic sites. Lately, the most employed approach consists of generating secondary porosity in zeolite structures, through several synthetic routes: removal of framework atoms, surfactant-assisted hydrothermal procedures in the presence of zeolite seeds, organosilane-based methods and crystallisation of the walls of amorphous aluminosilicate solids [6-9]. However, despite the massive scientific interest and the achieved progresses in this research field, the economic aspects, due to the use of more expensive procedures and reagents compared to conventional zeolites, combined with procedures rather time-consuming and difficult to control, have represented a strong limitation for real commercial applications.

The prevalent alternative method to obtain silica-based large-pore acid materials is to generate the acidic sites by the insertion of trivalent heteroelements (as Al^{3+} , Ga^{3+} , Fe^{3+} ,...) into the silica framework, with a consequent negative charge compensation by protons. Particularly, when Al atoms replace Si, surfactant-templated mesoporous silicas, like MCM-41, become active acidic catalysts for many reactions (cracking, isomerization and alkylation) [10-13]. The nature of the catalytic sites, in terms of coordination geometry, dispersion and stability, depends strongly on several synthesis parameters, such as Si/Al ratio, the source of aluminum used for the preparation, the pH conditions and the ageing temperature. Particularly, several studies have focused on the effect of varying aluminum sources and silicon-to-aluminum ratios on acid sites density and strength as well as catalytic properties [14-16].

The acidic properties tailoring of mesostructured aluminosilicates is a key-factor for their use as catalyst for a wide range of acid-catalyzed processes, but a true application on industrial scale still requires the overcoming of classical preparation processes, based on time-consuming and expensive steps. Therefore, the development of a cost-effective process for mesostructured aluminosilicates production is highly envisaged. To this purpose, the aerosol-based spray-drying method represents a simple and potentially scalable process to be adapted for the synthesis of surfactant-templated mesoporous systems. Besides these advantages, spray-drying processes allow a rather strict control of chemical and structural features of sprayed particles. The control of size and shape of particles by varying the spray-drying process parameters (*i.e.* feed rate, gas flow, temperature profile) and

synthesis conditions (*i.e.* alkoxide/surfactant ratio, precursor concentration, type of solvent) is an outstanding advantage of aerosol-assisted synthesis compared to classical preparation routes [17]. Mesoporous particles with spherical morphology are highly envisaged for diffusion-related applications, including catalysis, adsorption, separation and sensing. Several strategies have been investigated, with the aim of producing mesostructured silicas in the shape of spheres with adjustable sizes: among them, fluorine-promoted condensation [18], emulsion-based approach [19], hydrothermal co-condensation [20, 21] and transformation of preformed spheres of silica gel into micelle-template silica, known as pseudomorphic synthesis [22]. All these procedures, although successful, are conducted in batch operations, employing hydrothermal conditions and the use of additional reagents, which increase the production costs.

In the literature, the production of spherical mesoporous silica particles, characterized by high surface area and a well-defined internal porosity, by spraying hydrolyzed alkoxide/organosilane solutions containing surfactants, has been reported, showing the feasibility of the synthetic method [23-26]. Spray-drying is also an advantageous way to synthesise mesoporous silica spheres with high loading of heteroelements, leading to a wide range of functional properties, such as improved hydrothermal stability, bioactivity (calcium and/or phosphate incorporation) [27] and catalytic activity (Pt, Au, Zr and Al incorporation) [28]. For instance, very recently one-pot aerosol assisted sol-gel processes were successfully employed for synthesizing spherical super-microporous MoO₃-SiO₂-Al₂O₃ catalysts for high olefin metathesis activity [29, 30], as well as of bimetallic catalysts for hydrogenation reaction [31] and low temperature VOC oxidation [32].

Compared to traditional batch synthesis methods, aerosol-assisted approach allows the incorporation of high loading of heteroelement while maintaining uniform composition without phase segregation [28]. Within the large class of substituted mesoporous silicas, the synthesis by spray-drying process of aluminosilicate materials with high aluminium content have received sizable interest [33, 34]. However, these aerosol-assisted processes, although effective, are usually performed by spraying synthesis solution containing significant amount (up to *ca* 60% v/v) of inflammable solvents (mostly ethanol), which involves both safety and economic constraints in view of an effective manufacturing scale-up.

At variance in this work, aiming to deal with the needs of safety and waste disposal reduction required by a large-scale manufacture, the direct preparation of mesoporous aluminosilicates, with homogeneous spherical morphology and satisfactory yield, was obtained by spraying mild acidic aqueous synthetic solution. Two different aluminum sources have been used, fixing the silicon to aluminum nominal ratio, in order to investigate the influence on structural and acidic properties of the sprayed samples. The coordination of the incorporated aluminum has been studied by ²⁷Al-

NMR and the nature of acidic sites by FT-IR, both as the ability to transfer a proton to ammonia and through the perturbation of adsorbed CO. XRD, N₂ adsorption-desorption, FE-SEM and TEM, both coupled to EDX, analysis have revealed particles with micron-sized spherical shape, characterized by fully accessible and uniform network of pores.

2. Experimental section

2.1 Precursors solutions and aerosol-assisted processing: Aerosol-assisted syntheses were performed on a Mini Spray-Dryer B-290, Büchi. The heater inlet temperature was held constant at 493 K and the outlet temperature stayed constant at 398 K. The aspirator ran at a maximum air speed of 40 m³/h. The feeding speed was held constant at 5.1 mL/min and the N₂ gas flow was set at 670 L/h.

The synthesis solutions for spray-drying were prepared by modifying the recipe reported by Ide *et al.* [24] for micrometer sized spherical mesoporous silica particles through adding a proper amount of aluminum precursor to the synthesis mixture. In a typical synthesis, hexadecyltrimethylammonium bromide (99%, Aldrich) (CTAB) was dissolved in an HCl (37% w/w, Sigma) aqueous solution. TEOS (98%, Aldrich) and the aluminum precursor were mixed and sonicated prior to their addition, in a drop wise manner, to the surfactant solution. Aluminum isopropoxide (AIP, Al(C₃H₇O)₃; Aldrich; 99%) and aluminum chloride hexahydrate (AlCl₃ 6 H₂O, puriss., Sigma) were used as aluminum sources. The solutions were stirred for 1 hour before spray-drying. The composition of the sprayed mixtures were 1 TEOS : x Al(C₃H₇O)₃ (or AlCl₃* 6 H₂O) : 0.12 CTAB : 1400 H₂O : 1.5 HCl, where x = 0.01 and 0.05.

The sample prepared with AIP precursor will be referred as Al_ISO_10 (nominal Si/Al = 10) and Al_ISO_20 (nominal Si/Al = 20), whereas the sample prepared with aluminum chloride as Al_Cl_10 (Si/Al = 10) and Al_Cl_20 (Si/Al = 20).

The resulting powders were calcined under air at a heating rate of 1.0 K/min at 823 K and kept at this temperature for 6 h.

2.2 Characterization: The samples were characterized by X-ray diffraction (XRD) through a Philips X'pert diffractometer (Cu K α radiation) and nitrogen adsorption measurements at 77 K performed using a Quantachrome Autosorb 1. Samples were outgassed at 423 K for 5 hours before analysis. BET specific surface areas have been calculated in the relative pressure range 0.04–0.1 and the pore size has been evaluated through the DFT (Density Functional Theory) method, using the NLDFT equilibrium model for cylindrical pore [35]. Scanning electron microscopy (SEM) analyses were performed with a JEOL-JX-A8600. Transmission Electron Microscopy (TEM) was performed with a FEI Tecnai F20ST operating at 200 kV. The samples were dispersed in ultrapure ethanol after few

seconds of sonication in ultrasound bath and then a drop of this solution dispensed on TEM copper grid with holey carbon (200 mesh).

For FT-IR measurements, powders were pressed into thin, self-supporting wafers. FT-IR measurements were performed with a Bruker Equinox 5 spectrometer operating at 2 cm^{-1} resolution. Pre-treatments were carried out using a standard vacuum frame, in an IR cell equipped with KBr windows. Wafers were outgassed 1 hour at 573 K before adsorption of CO at nominal 77 K and ammonia at room temperature.

Nuclear magnetic resonance spectra of ^{27}Al with magic-angle spinning conditions were performed in a Bruker Advance III 500 spectrometer. The spectra were recorded by using $1.0\ \mu\text{s}$ single-pulse excitation (1H high power decoupling), corresponding to a flip angle of $\pi/20$ in order to ensure selective excitation of the central transition. A recycle delay of 0.5 s was used for all experiments. The spinning frequency was 15 kHz. Acid aqueous solution of aluminum nitrate (1 mol L^{-1}) was used as external reference.

3. Results and Discussion

3.1 Morphological and textural features of spray-dried aluminosilicates

Mesoporous aluminosilicates, with spherical morphology and high Al content, have been synthesized under mild acidic aqueous conditions by using an aerosol-assisted sol-gel process. Two aluminum sources, aluminum isopropoxide and aluminum chloride, have been used, keeping constant the other synthesis and process parameters in order to highlight the effect of the heteroatom precursor on the nature and distribution of the incorporated acidic sites in the final materials.

FE-SEM micrographs of the all synthesized sprayed powders show well-defined and smooth micrometric spheres, mostly ranging between $1\ \mu\text{m}$ and $2\ \mu\text{m}$, as shown in Figure 1a (Al_ISO_10) and Figure 1b (Al_Cl_10). FE-SEM images of Al_ISO_20 and Al_Cl_20 are reported as Supplementary Information (SI.1). For all samples no collapsed or broken spheres are observed, indicating that the surface tension of sprayed sols is sufficiently high to avoid a droplet deformation at the tip of the spray-dryer, favouring a spherical morphology [24].

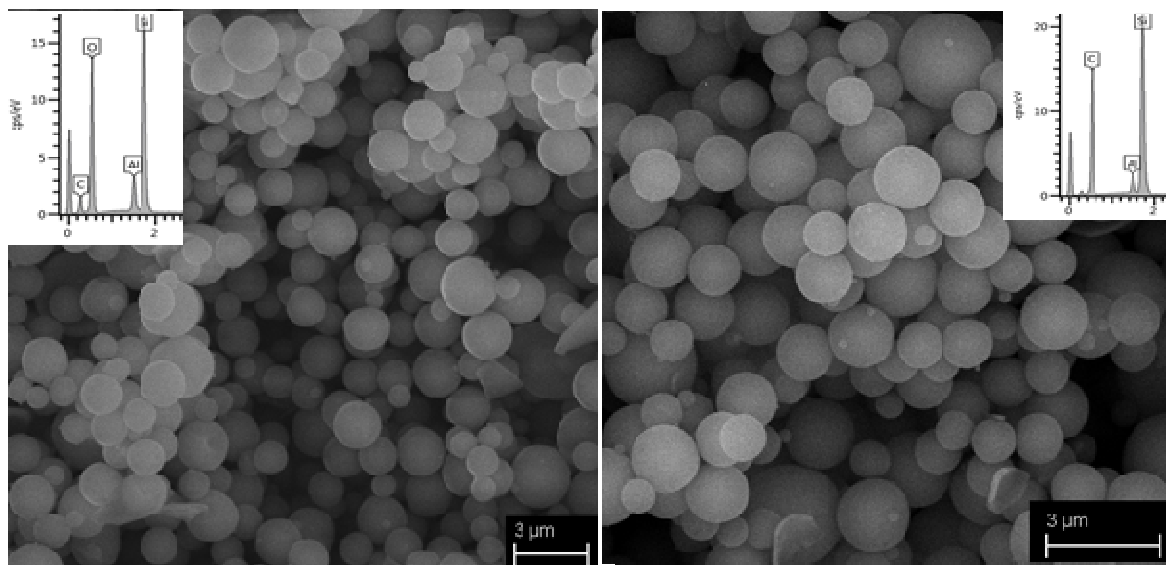


Figure 1: FE-SEM images and EDX spectra (insets) of sprayed Al_ISO_10 (section a) and Al_Cl_10 (section b).

EDX analysis confirms the presence of aluminum for all the analysed samples: the Si/Al ratio, as average of three measurements, is 5.7 for Al_ISO_10 and 14.3 for Al_ISO_20, i.e. lower than the nominal ratio for both samples. The values are 9.8 for Al_Cl_10 and 19.6 for Al_Cl_20, in fair agreement with the nominal ratios. The variance between the observed EDX and nominal ratios for samples prepared by isopropoxide precursor is likely to result from several factors.

It is widely reported in the literature that the Al isopropoxide, in combination with TEOS, as silica precursor, generally enhances the amount of aluminum incorporation in Al-modified mesoporous silicas compared to other sources [36, 37]. Under acidic conditions, aluminum isopropoxide hydrolyzes more rapidly than TEOS to soluble monomeric species $\text{Al}(\text{OH})_4^-$ [38], which, during the assembly mechanism, can establish, at variance with the protonated silica oligomers, direct electrostatic interactions with the cationic heads of template. Therefore, when Al isopropoxide is used as precursors, an enrichment of aluminum species at organic-inorganic interface is expected, leading to higher concentration of aluminum species inside the droplets generated by the atomizer and consequent preferential Al incorporation. This effect could lead to Al-rich areas inside the sprayed spheres, that for certain extent could justify the observed EDX Si/Al ratio. Furthermore, if it is assumed that not the total TEOS nominal amount is effectively converted to polymerized silica, as previously observed by the authors in aerosol processing of functionalized mesoporous silicas [25], a lower Si/Al ratio for the final materials is expected.

On the other hand, when the salt precursor is used, the aluminum species formed during hydrolysis are mainly the positively charged $[\text{Al}(\text{H}_2\text{O})_6^{3+}]$ and $[\text{Al}(\text{OH})(\text{H}_2\text{O})_5^{2+}]$ species, that are involved in Br^- mediated interaction with the ammonium groups in the same way as protonated silica precursors [39].

Figure 2 shows the XRD patterns of samples Al_ISO_10 (spectrum a) and Al_Cl_10 (spectrum b): a main intense peak at low 2θ values and a broad less intense reflection at higher 2θ values

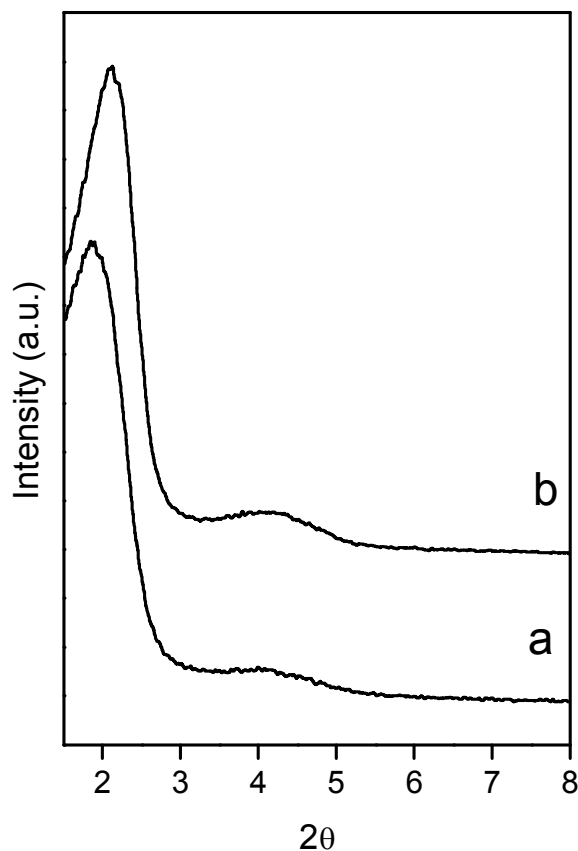


Figure 2: XRD patterns of calcined Al_ISO_10 (curve a) and Al_Cl_10 (curve b).

are observed for both samples. Compared to the typical diffraction pattern of CTAB-templated materials with hexagonal $p6mm$ phase, characterized by three distinct peaks indexed as (1 0 0), (1 1 0) and (2 0 0) reflections, sprayed samples show a less defined d_{100} peak and the presence of diffuse scattering instead of defined d_{110} and d_{200} peaks, usually ascribed to a decrease of the mesoscopic order. Nevertheless the presence of diffuse scattering instead of defined d_{110} and d_{200} peaks may be also due to the small size of locally ordered domains. Considering that the XRD pattern reported for sprayed CTAB-templated silica, prepared with a similar procedure [24] but without aluminum precursors, is that typical of hexagonally ordered mesophase, it appears that the low order mostly

results from the effect of the aluminum species on mesophase organization, as already known for equivalent materials obtained by sol-gel precipitation [40].

The basal d spacing, calculated on position of d_{100} reflection, results 4.7 nm for Al_ISO_10 and 4.1 nm for Al_Cl_10. These data show that when aluminum isopropoxide is used as precursor a higher d parameter is obtained.

Transmission electron microscopy analysis of both samples (Fig. 3) shows that the porosity is homogeneous throughout the spheres, in the form of a worm-like system of pores, which is in agreement with the low order evidenced by the XRD analysis.

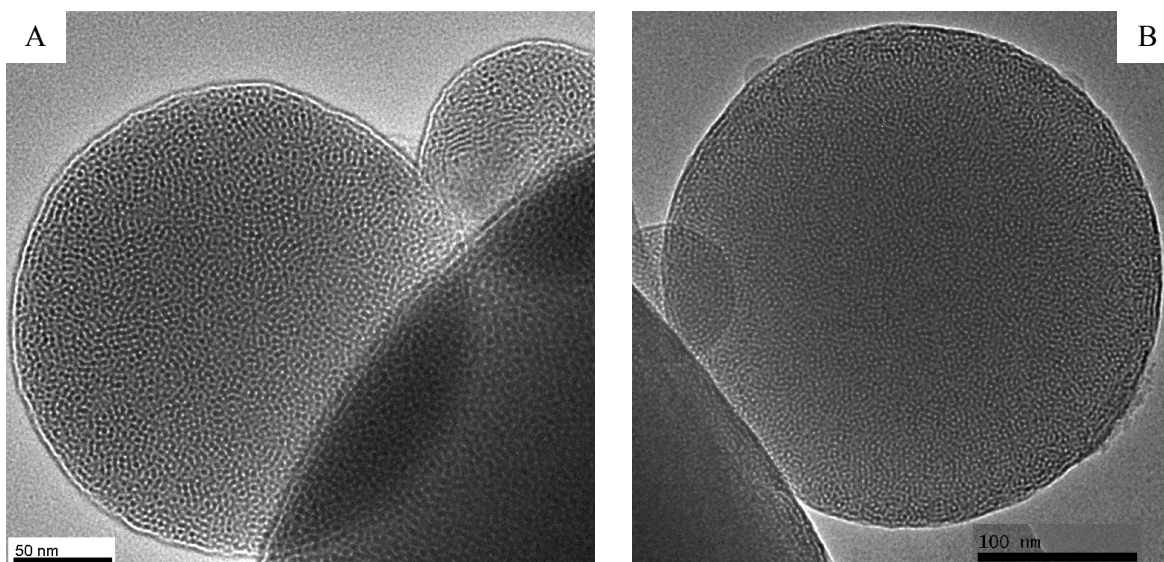


Figure 3: TEM image of calcined Al_ISO_10 (A) and Al_Cl_10 (B)

N_2 adsorption/desorption isotherms of spayed alluminosilicates are of type IV, exhibiting filling of the mesopores at relative pressure p/p_0 below 0.3. Figure 4 reports the curves related to Al_ISO_10 (curve a) and Al_Cl_10 (curve b), the curves related to the samples with higher Si/Al ratio are reported in SI.2. The calculated values of BET specific surface areas, mesopore volumes and DFT pores diameter are reported in Table 1.

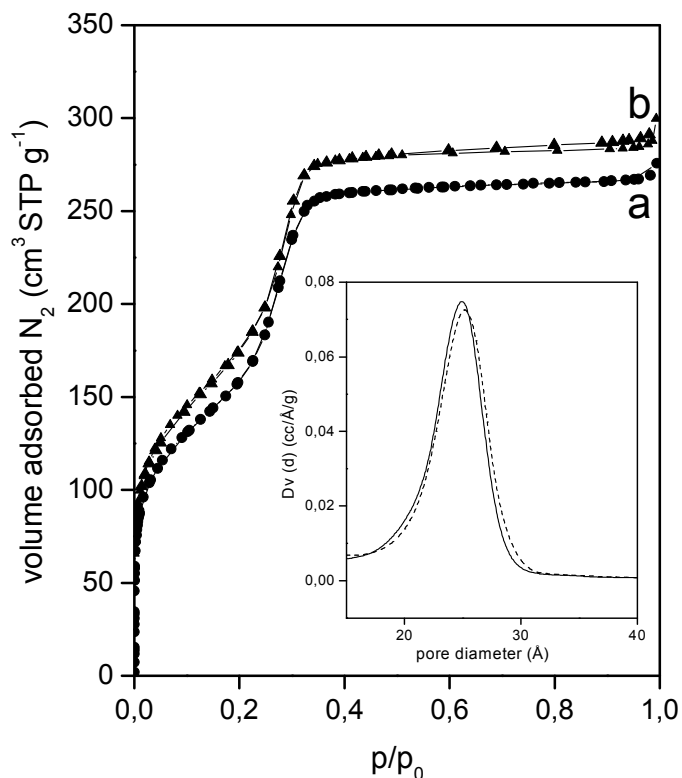


Figure 4: Nitrogen adsorption isotherms of Al_ISO_10 (curve a) and Al_Cl_10 (curve b). Inset: DFT pore size distributions calculated for Al_ISO_10 (solid curve) and for Al_Cl_10 (dashed curve).

Table 1: Textural parameters obtained from N₂ adsorption-desorption isotherms

	SSA _{BET} (m ² /g)	V _p (cm ³ /g)	D _{DFT} (nm)
Al_ISO_10	602	0.43	2.5
Al_Cl_10	642	0.46	2.5
Al_ISO_20	648	0.46	2.5
Al_Cl_20	660	0.48	2.5

Al_ISO_10 and Al_Cl_10 before calcination were also studied by ²⁷Al-MAS-NMR in order to investigate the coordination of incorporated aluminum atoms. ²⁷Al-MAS-NMR spectra of both samples are reported in Figure 5. An intense peak, due to tetrahedral coordinated aluminum, is

observed for both systems at around 54 ppm, in fair agreement with reported chemical shifts assigned to tetrahedral species in aluminum containing mesoporous silica and zeolites [41, 42].

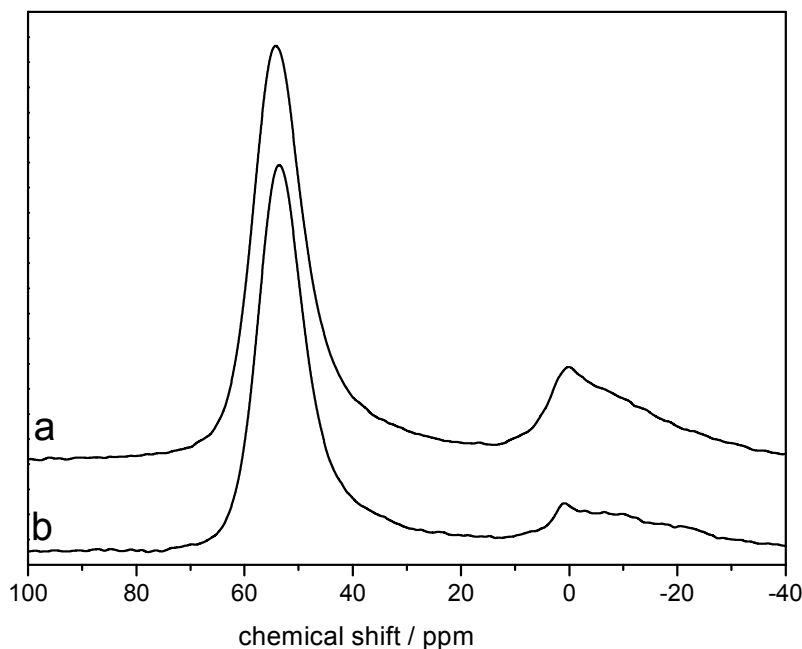


Figure 5: ^{27}Al -MAS-NMR spectra of (a) Al_ISO_10 and (b) Al_Cl_10.

Octahedral aluminum (peak at *ca* 0 ppm) in minor amounts was also observed and can be attributed to extra-framework aluminum or to partially extra-framework species [43].

The ratios between the areas of the resonance peaks related to tetrahedral and octahedral aluminum are 2.0 and 2.8, respectively for Al_ISO_10 and Al_Cl_10.

3.2. Acidic properties of spray-dried alluminosilicate

The Brønsted and Lewis acidity of the Al-containing samples produced by aerosol processing were investigated by following in the IR the interaction with ammonia and carbon monoxide, a strong and weak base, respectively, able to interact with both acidic hydroxyl groups (Brønsted sites) and coordinatively unsaturated cations (Lewis sites).

For sake of brevity, the spectra of adsorbed NH_3 and CO adsorbed on Al_ISO_10 and Al_Cl_10 will be reported and discussed, being very similar the behaviour shown by the homologues samples with lower Al content (Al_ISO_20 and Al_Cl_20).

The FT-IR spectra of samples treated under vacuum at 573 K in the OH-stretching region (Figure 6) show very similar features: a prominent peak at about 3740 cm^{-1} , assigned to the OH stretching vibration of isolated silanol groups, and a broad and intense absorption in the $3700\text{--}3000\text{ cm}^{-1}$, due to hydroxyls interacting via H-bonding. Brønsted acidity of surface -OH species has been studied as the propensity of -OH species to either protonate ammonia or engage in H-bond with carbon monoxide.

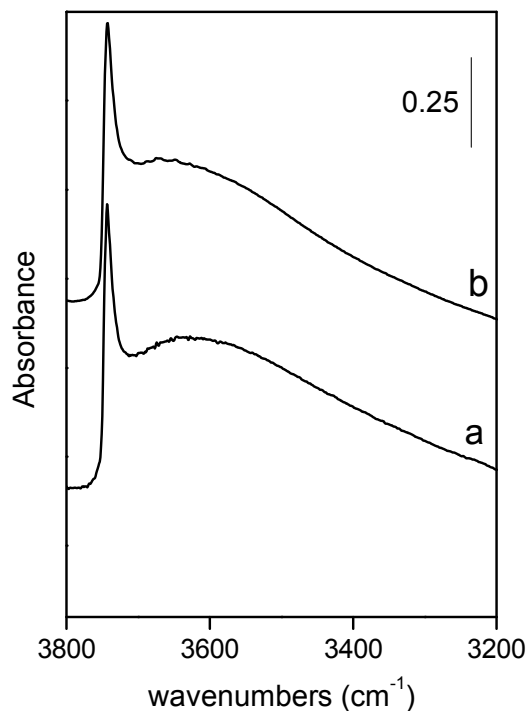


Figure 6: IR spectra ($3800\text{--}3000\text{ cm}^{-1}$) of Al_ISO_10 (curve a) and Al_Cl_10 (curve b) outgassed at 573 K.

Figure 7 reports results concerning the adsorption of NH_3 on both samples: curves a and b represent respectively the spectra (normalized with respect to weight) of Al_ISO_10 and Al_Cl_10, both outgassed at 573 K, after ammonia adsorption and prolonged outgassing at RT. A band at about 1450 cm^{-1} is observed for both samples, which is a clear evidence that -OH species acidic enough to transfer their protons to ammonia are present. The intensity of the band due to ammonium species for Al_ISO_10 is almost two-fold that found for Al_Cl_10; assuming fairly constant the related extinction coefficient for the ammonium species in the two samples, it results that a higher amount of Brønsted sites, able to transfer their protons to ammonia, is present in Al_ISO_10. This is in line with the higher amount of incorporated aluminum for Al_ISO_10 as evidenced by EDX analysis.

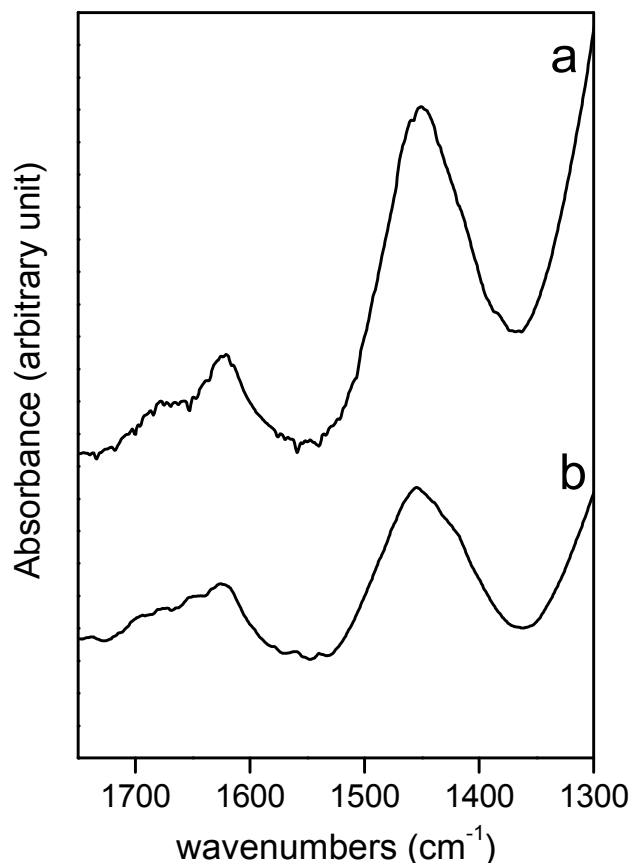


Figure 7: IR spectra recorded on Al_ISO_10 (a) and Al_Cl_10 (b) outgassed at 573 K after ammonia adsorption and prolonged evacuation at RT.

The less intense band at about 1625 cm^{-1} is assigned to NH_3 molecules, probably adsorbed on Al^{3+} Lewis sites.

Results of adsorption of ammonia on Al_ISO_20 and Al_Cl_20 (Figure SI.3) are in line with previous ones, confirming a lower amount of Brønsted sites in Al_Cl_20 compared to Al_ISO_20, in fair agreement with the detected Si/Al ratios.

In order to investigate more extensively the Brønsted and the Lewis acidic sites probed by ammonia, FT-IR spectra of adsorbed carbon monoxide have been also registered. Figure 8.A shows the difference spectra (spectrum of naked sample outgassed at 573 K has been subtracted) in the $2250\text{-}2050\text{ cm}^{-1}$ range of CO adsorbed on Al_ISO_10. Upon low CO pressures a band centred at about 2169 cm^{-1} grows first, shifting progressively to 2158 cm^{-1} with increasing coverage. To investigate further the nature of the band observed at low coverage, a simulation of the envelope in the $2190\text{-}2140\text{ cm}^{-1}$ range, registered at the CO equilibrium pressure of 0.5 mbar, has been attempted by using two bands whose frequency and half-height width have not been forced. The analytical form of each peak was assumed to be a Gaussian. The best fitting is reported in the inset

of Figure 8.A and shows two components: one, more intense, at 2163 cm^{-1} and the other at 2172 cm^{-1} . The former is, coherently with the literature, attributed to CO interacting with acidic Al-OH species, similar to those formed in zeolites by incipient dealumination [44] and on ITQ-2 system [45]. The latter, at higher frequency, is assigned to CO interacting with weak Lewis Al sites, as reported for Al-MCM-41 systems [46, 47], where aluminum is supposed intruded into the amorphous structure of the walls and thus partially shielded by neighbouring hydroxyls groups. The band at 2158 cm^{-1} , observed at higher coverage, is assigned to CO molecules interacting with free silanols [37].

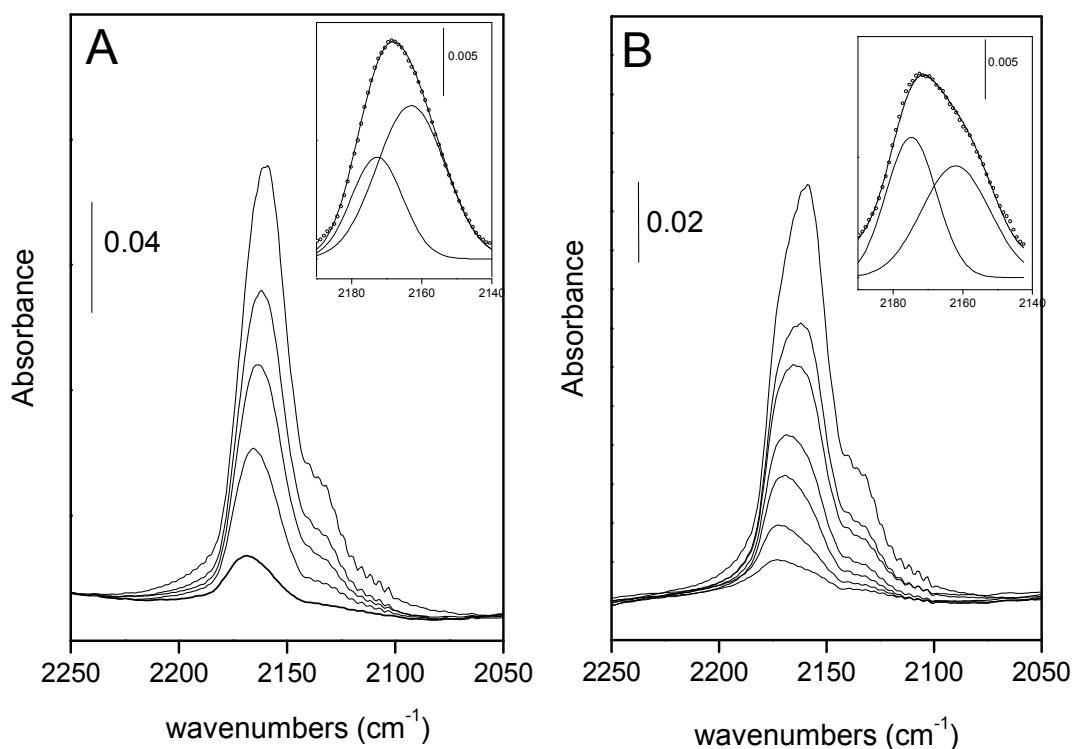


Figure 8: IR difference spectra ($2250\text{--}2050\text{ cm}^{-1}$) of CO adsorbed at nominal 77 K on Al-Cl-ISO outgassed at 573 K (section A) and on Al-Cl-10 outgassed at 573 K (section B). Insets for both sections: simulation of the spectrum registered in presence of 0.5 mbar CO, in the $2190\text{--}2140\text{ cm}^{-1}$ range.

No band at 2230 cm^{-1} usually assigned to coordinatively unsaturated tetrahedral Al^{3+} [48] was observed.

Figure 8.B reports the difference spectra of CO adsorbed on Al-Cl-10, previously activated at 573 K. The most significant difference is that the band growing at low CO coverage is centred at

slightly higher frequency (*ca* 2173 cm^{-1}) with respect to Al_ISO_10. The simulation of the band (reported in the inset), registered upon equal CO equilibrium pressure as before, reveals two components: the first at 2174 cm^{-1} and the second at 2163 cm^{-1} . Although, essentially, the same species found for Al_ISO_10 are detected for this sample, it is worthy to note that at low coverage the band ascribed to CO interacting with acidic Al-OH species is less intense compared with the signal ascribed to CO on Al^{3+} sites, which is coherent with the lower amount of Brønsted sites detected by ammonia.

Support to the proposed assignment comes from the inspection of the difference spectra in the high frequency region (3800-3200 cm^{-1}) registered at low CO coverage. Figure 9 shows to the difference spectra in the O-H stretch region of Al_Cl_ISO outgassed at 573 K (curve a) and of Al_Cl_10 outgassed at 573 K (curve b) in contact with 0.5 mbar CO: a clear negative band centred at about 3670 cm^{-1} , is observed for both spectra (arrows) paired with a band growing at *ca* 3465 cm^{-1} .

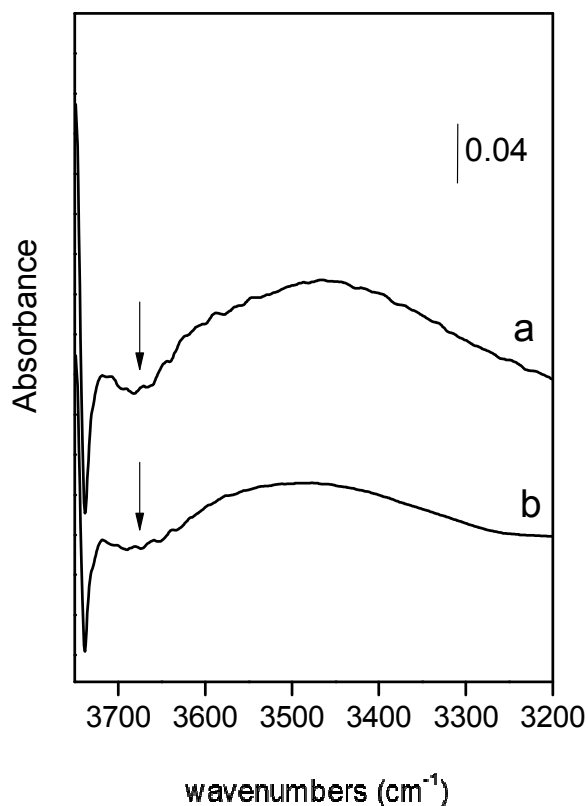


Figure 9: IR difference spectra in the O-H stretching region (3800–3200 cm^{-1}) of CO adsorbed (low coverage) on Al_Cl_ISO outgassed at 573 K (curve a) and on Al_Cl_10 outgassed at 573 K (curve b).

Hydroxyl groups absorbing at the observed frequency, able to suffer a $\Delta\nu_{\text{OH}}$ of about 200 cm^{-1} upon CO interaction and to protonate ammonia, have been attributed to considerably acid Al-OH species, similar to those formed in zeolites by incipient dealumination or in transition alumina [45, 47].

4. Conclusions

A fast and sustainable aerosol-assisted sol-gel process under mild acidic condition has allowed the direct synthesis of mesoporous aluminosilicates with high Al content, characterized by homogenous spherical particles, high surface area and accessible porosity. On equal synthesis and spraying procedure, the use of aluminum isopropoxide as precursor has led to higher amount of incorporated Al, compared with the use of aluminum chloride, most likely due to different hydrolysis rates and products of the two precursors. NMR analysis has confirmed that incorporated Al atoms in as-synthesized samples are mostly in tetrahedral coordination, suggesting that higher loadings can be obtained without phase segregation. FT-IR measurements of CO and NH_3 adsorption on samples outgassed at 573 K have shown the presence of Brønsted acidic sites, ascribed to Al-OH species able to protonate ammonia, and the presence of weak Lewis sites assigned to Al^{3+} species buried in the amorphous walls of the aluminosilicate.

Acknowledgments

Bionica Tech is kindly acknowledged for the use of the Mini-Spray-Dryer.

The authors thank Dr. Geo Paul and Prof. Leonardo Marchese of the Eastern Piedmont University for ^{27}Al NMR measurements.

References

- [1] R.A. Sheldon and H. Van Bekkum, *Fine Chemicals through Heterogeneous Catalysis*, WILEY-VCH, Verlag, GmbH, 2001
- [2] D. Brunel, A.C. Blanc, A. Galarnau, F. Fajula, *Catal. Today*, 2002, **73**, 139.
- [3] A. Corma, *Chem Rev*, 1995, **95**, 559.
- [4] Q. Cui, Y. Zhou, Q. Wei, X. Tao, G. Yu, Y. Wang, J. Yang, *Catalysts Energy Fuels*, 2012, **26**, 4664.
- [5] A.M. Alsobaai, R. Zakaria, B.H. Hameed, *Fuel Process. Tech.*, 2007, **88**, 921.
- [6] Y. Tao, H. Kanoh, L. Abrams, K. Kaneko, *Chem. Rev.*, 2006, **106**, 896.
- [7] Z. Zhang, Y. Han, F.S. Xiao, S. Qiu, L. Zhu, R. Wang, Y. Yu, Z. Zhang, B. Zou, Y. Wang, H. Sun, D. Zhao, Y. Wei, *J. Am. Chem. Soc.*, 2001, **123**, 5014.
- [8] L. Prokesova, S. Mintova, J. Cejka, T. Bein, *Mat. Sci. Eng. C-Bio S.*, 2003, **23**, 1001.

- [9] D.P. Serrano, R. Sanz, P. Pizarro, I. Moreno, *App. Catal. A: General*, 2012, **435**, 32.
- [10] A. Corma, V. Fornés, M.T. Navarro, J. Pérez-Pariente, *J. Catal.* 1994, **148**, 569.
- [11] A. Corma, A. Martínez, V. Martínez-Soria, J.B. Monton, *J. Catal.*, 1995, **153**, 25.
- [12] A. Corma, M.S. Grande, V. Gonzalez-Alfaro, A.V. Orchilles, *J. Catal.* 1996, **159**, 375.
- [13] J.J. Chiu, D.J. Pine, S.T. Bishop, B.F. Chmelka, *J. Catal.*, 2004, **221**, 400-412.
- [14] J.P. Lourenco, A. Fernandes, C. Henriques, M.F. Ribeiro, *Microp. Mesop. Mater.*, 2006, **94**, 56.
- [15] M.R. Carrott, F.L. Conceição, J.M. Lopes, P.J.M. Carrott, C. Bernardes, J. Rocha, F. Ramo, Ribeiro, *Microp. Mesop. Mater.*, 2006, **92**, 270.
- [16] B. Lindlar, A. Kogelbauer, R. Prins, *Microp. Mesop. Mater.* 2000, **38**, 167.
- [17] A. Bayu, D. Nandiyanto, K. Okuyama, *Adv. Powder. Tech.*, 2011, **22**, 1.
- [18] C. Boissière, A. Van der Lee, A. El Mansouri, A. Larbot, E. Prouzet, *Chem. Commun.* 1999, 2047.
- [19] Q. Huo, J. Feng, F. Schuth, D. G. Stucky, *Chem. Mater.*, 1997, **9**, 14.
- [20] A. Schlossbauer, M. A. Sauer, V. Cauda, A. Schmidt, H. Engelke, J. Rädler, U. Rothbauer, K. Zolghadr, C. Bräuchle, T. Bein, *Adv. Healthcare. Mater.*, 2012, **1**, 316.
- [21] C. Argyo, V. Cauda, H. Engelke, J. Rädler, T. Bein, *Chem. Eur. J.*, 2012, **18**, 428.
- [22] A. Galarneau, Iapichella, K. Bonhomme, F. Di Renzo, P. Kooyman, O. Terasaki, F. Fajula, *Adv. Funct. Mater.* 2006, **16**, 1657.
- [23] N. Andersson, P.C. Alberius, S.J. Pedersen, L. Bergström, *Micropor. Mesopor. Mater.* 2004, **72**, 175.
- [24] M. Ide, E. Wallaert, I. Van Driessche, F. Lynen, P. Sandra, P. Van Der Voort, *Microp. Mesop. Mater.*, 2011, **142**, 282.
- [25] S. Fiorilli, F. Tallia, L. Pontiroli, C. Vitale-Brovarone, B. Onida, *Materials Letters*, 2013, **108**, 118.
- [26] I.V. Melnyk, M. Fatnassi, T. Cacciaguerra, Y. Zub, B. Alonso, *Micropor. Mesopor. Mater.* 2012, **152**, 172.
- [27] D. Arcos, A. López-Noriega, E. Ruiz-Hernández, O. Terasaki, M. Vallet-Regí, *Chem. Mater.* 2009, **21**, 1000.
- [28] C. Boissiere, D. Grosso, A. Chaumonnot, L. Nicole, C. Sanchez, *Adv. Mater.*, 2011, **23**, 599.
- [29] D.P. Debecker, M. Stoyanova, F. Colbeau-Justin, U. Rodemerck, C. Boissière, E. M. Gaigneaux, C. Sanchez, *Angew. Chem. Int. Ed.* 2012, **51**, 2129.
- [30] S. Maksasithorn, P. Praserttham, K. Suriye, D. P. Debecker, *Microp. Mesop. Mater.* 2015, **213** 125.

- [31] F. Colbeau-Justin, C. Boissière, A. Chaumonnot, A. Bonduelle, C. Sanchez, *Adv. Funct. Mater.* 2014, **24**, 233.
- [32] C. Y. Wang, H. Bai, *Catalysis Today*, 2011, **174**, 70.
- [33] S. Pega, C. Boissiere, D. Grosso, A. Chaumonnot, L. Nicole, C. Sanchez, *Angew. Chem. Int. Ed.*, 2009 **48**, 2784.
- [34] A. Chaumonnot, F. Tihay, A. Coupé, S. Pega, C. Boissière, D. Grosso, C. Sanchez, *Oil & Gas Sci Tech.*, 2009, **64**, 681.
- [35] M. Thommes, R. Kohn, M. Froba, *Appl. Surf. Sci.* 2002, **196**, 239.
- [36] M. Hartmann, C. Bischof, *Stud. Surf. Sci. Catal.* 1998, **117**, 249.
- [37] A. Vinu, V. Murugesan, W. Böhlmann, M. Hartmann, *J. Phys. Chem. B* 2004, **108**, 11496.
- [38] Y. Li, W. Zhang, L. Zhang, Q. Yang, Z. Wei, Z. Feng, C. Li, *J. Phys. Chem. B*, 2004, **108**, 9739.
- [39] C.J Brinker, G.W. Scherer, *Sol-gel science*, Academic Press, INC, 1990
- [40] R. Mokaya, *J. Phys. Chem. B*, 2000, **104**, 8279
- [41] S. Wu, Y. Han, Y.C Zou, J.W. Song, L. Zhao, Y. Di, S.Z. Liu, F.S. Xiao, *Chem. Mater.*, 2004, **16**, 486.
- [42] R. Mokaya, *Chem. Comm.*, 1997, 2185.
- [43] C. Bisio, G. Martra, S. Coluccia, P. Massiani, *J. Phys. Chem. C*, 2008, **112**, 10520.
- [44] L.M. Kustov, V.B. Kasansky, S. Beran, L. Kubelková, P. Jiru, *J. Phys. Chem.*, 1987, **91** (20), 5247
- [45] B. Onida, L. Borello, B. Bonelli, F. Geobaldo, E. Garrone, *J. Catal.*, 2003, **214**, 191.
- [46] A. Katovic, G. Giordano, B. Bonelli, B. Onida, E. Garrone, P. Lentz, J.B. Nagy, *Micropor. Mesopor. Mater.*, 2001, **44**, 275.
- [47] B. Bonelli, B. Onida, J.D. Chen, A. Galarneau, F. Di Renzo, F. Fajula, E. Garrone, *Microp. Mesop. Mater.*, 2004, **67**, 95.
- [48] O. Cairon, T. Chevreau, J.C. Lavalley, *J. Chem. Soc Faraday. Trans.*, 1998, **19**, 3039.

Graphical Abstract

Spray-dried mesoporous aluminosilicate, with spherical morphology, high surface area and accessible porosity, have been synthesized under mild acidic aqueous conditions by using different aluminum precursors.

